Supporting information

Eumitrins F-H: Three new Xanthone Dimers From The Lichen *Usnea baileyi* and Their Biological Activities

Van-Kieu Nguyen[a,b,*], Hoai-Vu Nguyen-Si[a,b], Asshaima Paramita Devi[c,d], Pakarapon Poonsukkho[e], Ek Sangvichien[e], Thanh-Nha Tran[f], Yusuke Hioki[g], Tohru Mitsunaga[h] and Warinthorn Chavasiri[c,*]

[a]*Institute of Fundamental and Applied Sciences, Duy Tan University, Ho Chi Minh City, Vietnam;*

[b]*Faculty of Natural Sciences, Duy Tan University, Da Nang, Vietnam;*

[c]*Center of Excellence in Natural Products Chemistry, Department of Chemistry, Faculty of Science, Chulalongkorn University, Pathumwan, Bangkok 10330, Thailand*

[d]*Program of Biotecnology, Faculty of Science, Chulalongkorn University, Pathumwan, Bangkok 10330, Thailand*

[e]*Lichen Research Unit and Lichen Herbarium, Department of Biology, Faculty of Science, Ramkhamhaeng University, Bangkapi, Bangkok 10240, Thailand*

[f]*Department of Enviromental Engineering, Thu Dau Mot University, Binh Duong, Vietnam*

[g]*Graduate School of Natural Science and Technology, Gifu University, 1-1 Yanagido, Gifu 501-1193, Japan*

[h]*Faculty of Applied Biological Sciences, Gifu University, 1-1 Yanagido, Gifu 501-1193, Japan*

[*] Correspondence: nguyenvankieu2@duytan.edu.vn, warinthorn.c@chula.ac.th

Abstract

The lichen *Usnea baileyi* is a fruticose lichen belonging to the *Usnea* genus. It is well known as a rich source of natural xanthone dimers and possesses various bioactivities. Nevertheless, the chemical investigation on this type of lichen is still rare as most of researches reported its components without structural elucidation. Herein, in the continuous study on this type of lichen, we further isolate xanthone dimers from the dichloromethane extract and explore three new xanthone dimers, eumitrins F−H (**1**−**3**). Their structures were elucidated unambiguously by spectroscopic analyses, including high resolution electrospray ionisation mass spectrometry (HRESIMS), 1D and 2D nuclear magnetic resonance spectroscopy (1D and 2D NMR), and DP4 probability. All compounds were evaluated for their enzyme inhibition against α-glucosidase, tyrosinase, and antibacterial activity. They revealed moderate antimicrobial and weak tyrosinase inhibition. For α-glucosidase inhibition, compound **3** displayed the most significant inhibitory against α-glucosidase possessing an IC_{50} value of 64.2 µM.

Table S1. ^{1}H (400 MHz) and ^{13}C (100 MHz) NMR Data for **1**−**3** ($CDCl_3$)

	1		**2**		**3**	
	δ_H (*J*, Hz)	δ_C	δ_H (*J*, Hz)	δ_C	δ_H (*J*, Hz)	δ_C
1		159.5		159.6		159.5
2		117.8		117.8		117.9
3	7.48, 1H, d, 8.4	141.1	7.47, 1H, d, 7.6	141.0	7.27, 1H, d, 8.0	140.3
4	6.58, 1H, d, 8.4	107.6	6.58, 1H, d, 8.4	107.5	6.61, 1H, d, 8.0	108.0
4a		157.3		157.3		157.5
5	3.89, 1H, d, 6.8	74.0	3.89, 1H, d, 6.8	74.0	4.18, 1H, brs	71.5
6	2.06, 1H, m	36.0	2.07, 1H, m	36.0	2.18, 1H, m	28.7
7	1.83, 1H, m 1.29, 1H, m	27.3	1.80, 1H m 1.29, 1H, m	27.2	2.54, 1H, dd, 18.4, 11.2 2.40, 1H, dd, 16.4, 4.0	32.8
8	2.24, 1H, m 1.75, 1H, m	21.5	2.20, 1H, m 1.73, 1H, m	21.4		179.7
8a	3.40, 1H, s	46.4	3.39, 1H, m	46.3		100.4
9		198.7		198.7		188.1
9a		106.8		106.8		107.2
10a		85.6		85.6		85.0
11	1.11, 3H, d, 6.8	17.7	1.11, 3H, d, 6.8	17.7	1.19, 3H, d, 6.4	17.7
12		170.1		170.2		169.9
13	3.84, 3H, s	53.3	3.83, 3H, s	53.3	3.70, 3H, s	53.7
1'		159.5		159.0		162.3
2'		117.8		117.6	6.50, 1H, s	111.4
3'	7.48, 1H, d, 8.4	141.1	7.49, 1H, d, 8.0	140.4		150.5
4'	6.58, 1H, d, 8.4	107.6	6.62, 1H, d, 8.8	107.4		115.8
4a'		157.3		159.0		156.2
5'	3.89, 1H, d, 6.8	74.0	3.73, 1H, d, 10.4	80.3	5.44, 1H, brs	66.3
6'	2.06, 1H, m	36.0	1.84, 1H, m	34.3	2.01, 2H, m	23.6
7'	1.83, 1H, m 1.29, 1H, m	27.3	1.96, 1H, m 1.23, 1H, m	31.2	2.54, 1H, m 2.40, 1H, m	22.0
8'	2.24, 1H, m 1.75, 1H, m	21.5	2.17, 2H, m	20.4	7.30, 1H, brs	141.7
8a'	3.40, 1H, s	46.4	2.99, 1H, dd, 11.6, 4.4	51.2		129.1
9'		198.7		197.4		184.9
9a'		106.8		107.6		105.8
10'		85.6		87.6		81.0
11'	1.11, 3H, d, 6.8	17.7	1.11, 3H, d, 6.8	18.4	2.08, 3H, s	21.3
12'		170.1		169.3		171.4
13'	3.84, 3H, s	53.3	3.68, 3H, s	53.0	3.78, 3H, s	53.8
14'						169.2
15'					1.82, 3H, s	20.5
1-OH	12.21, 1H, s		12.19, 1H, s		11.60, 1H, s	
8-OH						
1'-OH	12.21, 1H, s		11.88, 1H, s		12.01, 1H, s	

Table S2. Calculated data for **3a** and **3b** conformers, including the Boltzmann distribution from GFNn-xTB methods and ^{13}C NMR assignment from DP4+ and J-DP4 probability theories.

Conformer	Boltzmann distribution (%)	DP4+ probability (%)	J-DP4 probability (%)
3a1	31.763	0.39	2.15
3a2	31.891	0.39	2.14
3a3	36.347	0.42	2.20
3a (ave.)	100.0	7.24	16.41
3b1	12.382	46.03	37.11
3b2	12.421	46.35	37.75
3b3	17.777	0.41	1.39
3b4	18.129	3.17	8.83
3b5	6.344	-	-
3b6	6.346	-	-
3b7	9.108	-	-
3b8	17.492	2.84	8.44
3b (ave.)	78.201	92.76	83.59

Table S3. Enzyme inhibitory and antibacterial activity of **1-3**.

Samples	IC_{50} (μM)	MIC (μg/mL)

	α-Glucosidase	Tyrosynase	*E. coli* ATCC25922	*P. aeruginosa* ATCC27853	*S. aureus* ATCC25923	*B. subtilis* ATCC6633	*C. albicans* TISTR
1	>200	>200	62.5	250	500	62.5	250
2	>200	>200	125	250	500	62.5	125
3	64.2 ± 0.51	>200	250	250	125	N.d	250
Acarbose	93.6 ± 0.49						
Kojic acid		36.1 ± 1.07					
Chloramphenicol			9.76	31.25	19.53	4.88	250

N.d: Not detected

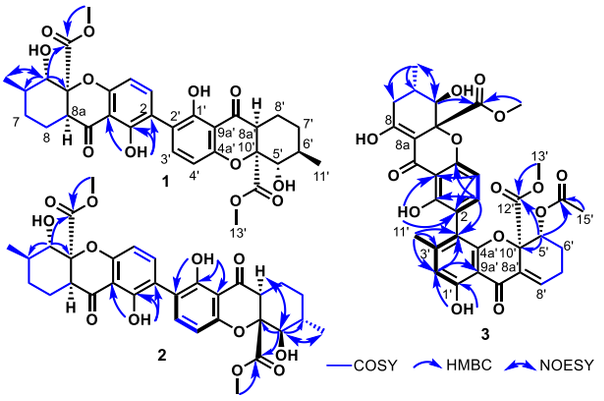

Fig. S1. . Selected COSY, HMBC and NOESY correlations of **1**–**3**.

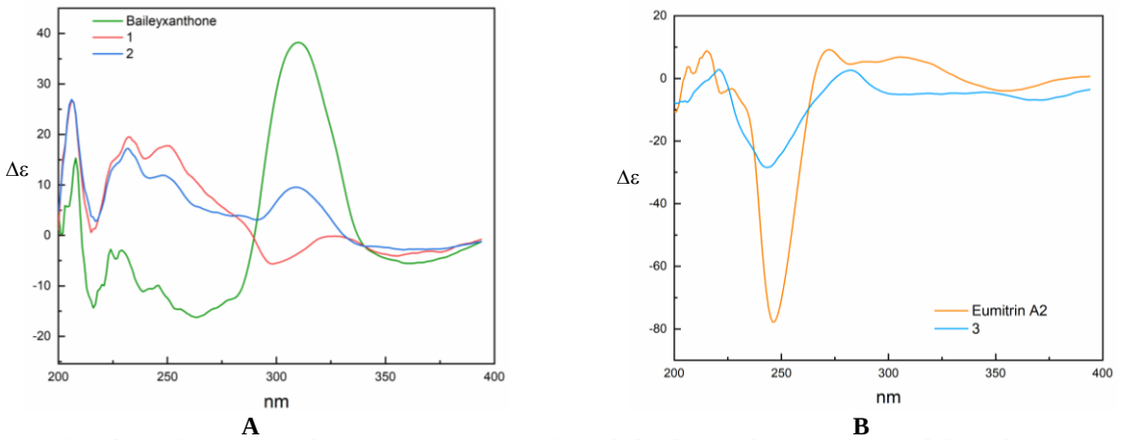

A **B**

Fig. S2. The ECD spectral comparison of **1**, **2** with bailexanthone (**A**); and **3** with eumitrin A2 (**B**).

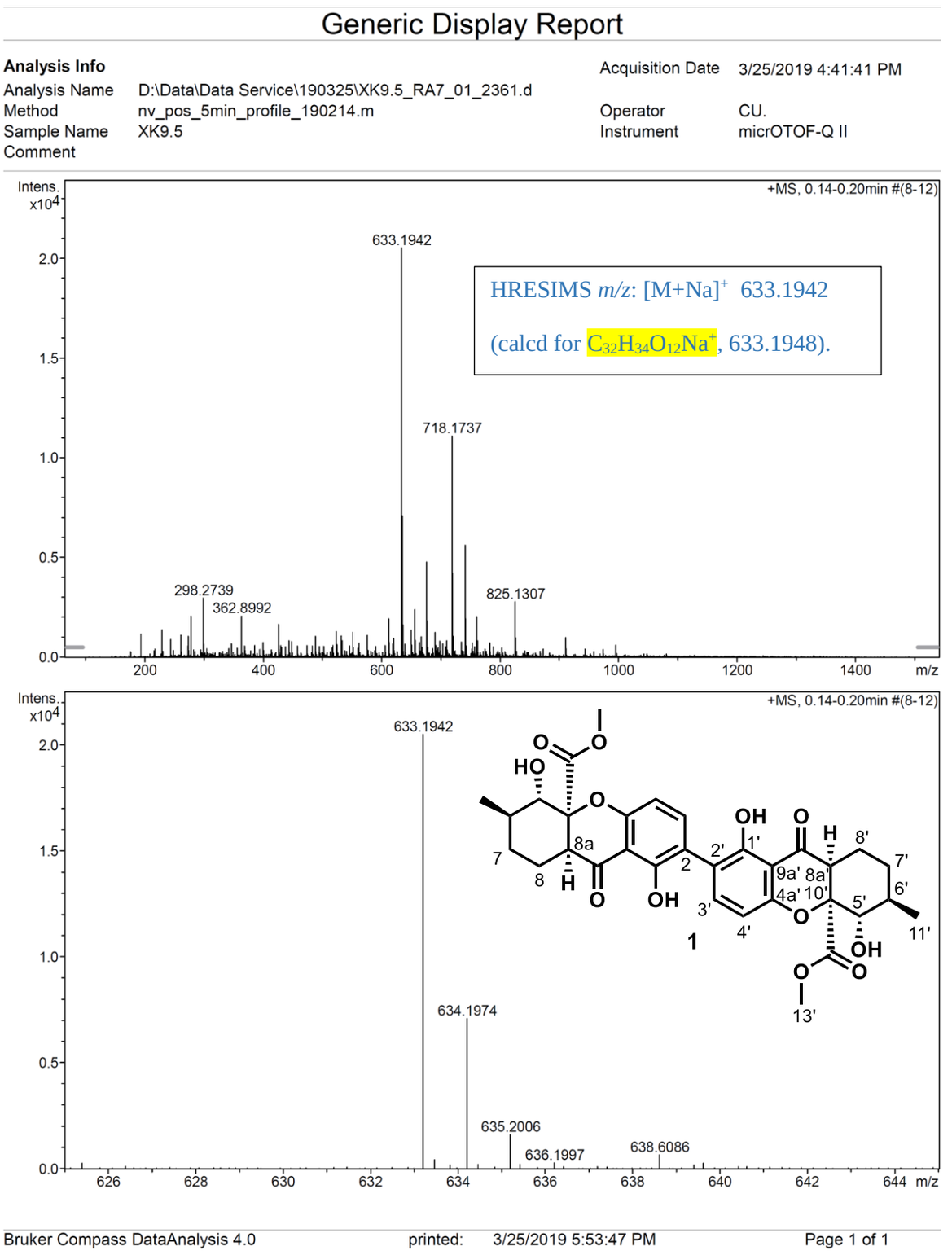

Fig. S3. The HRESIMS spectrum of **1**.

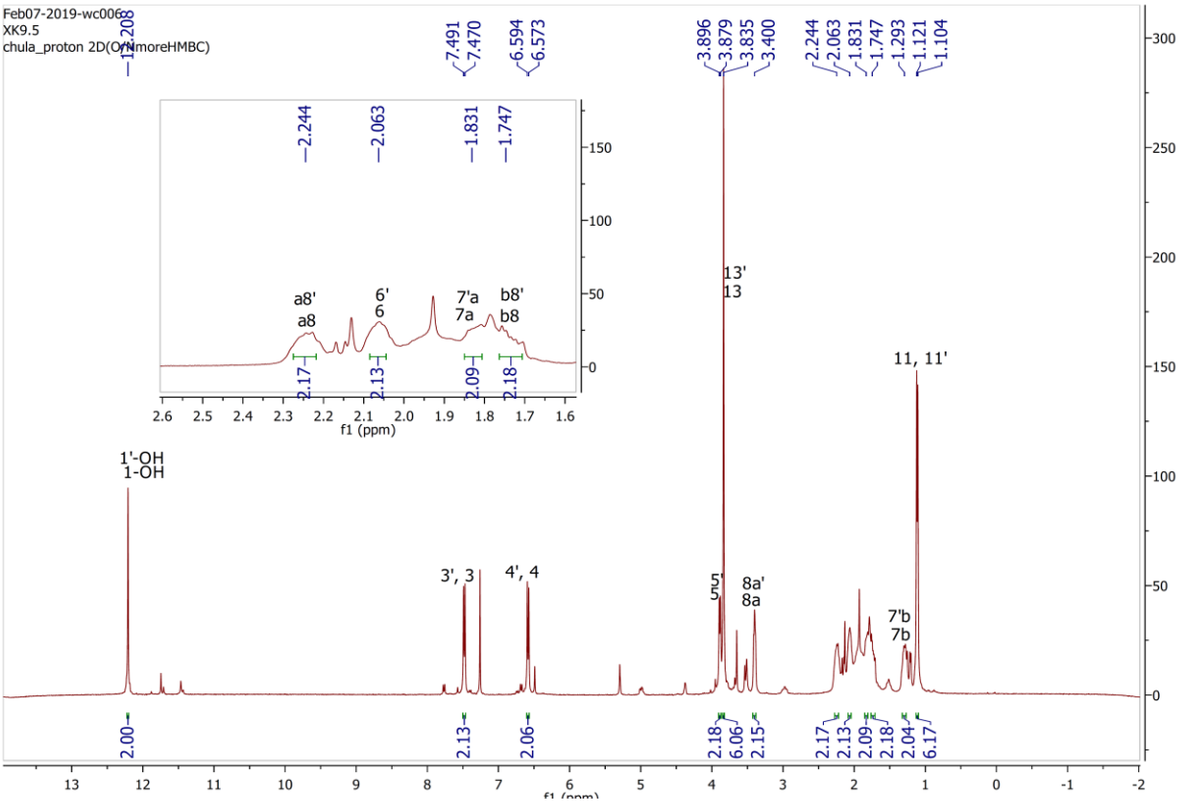

Fig. S4. The ^{1}H NMR spectrum of **1** in $CDCl_3$, 400 MHz.

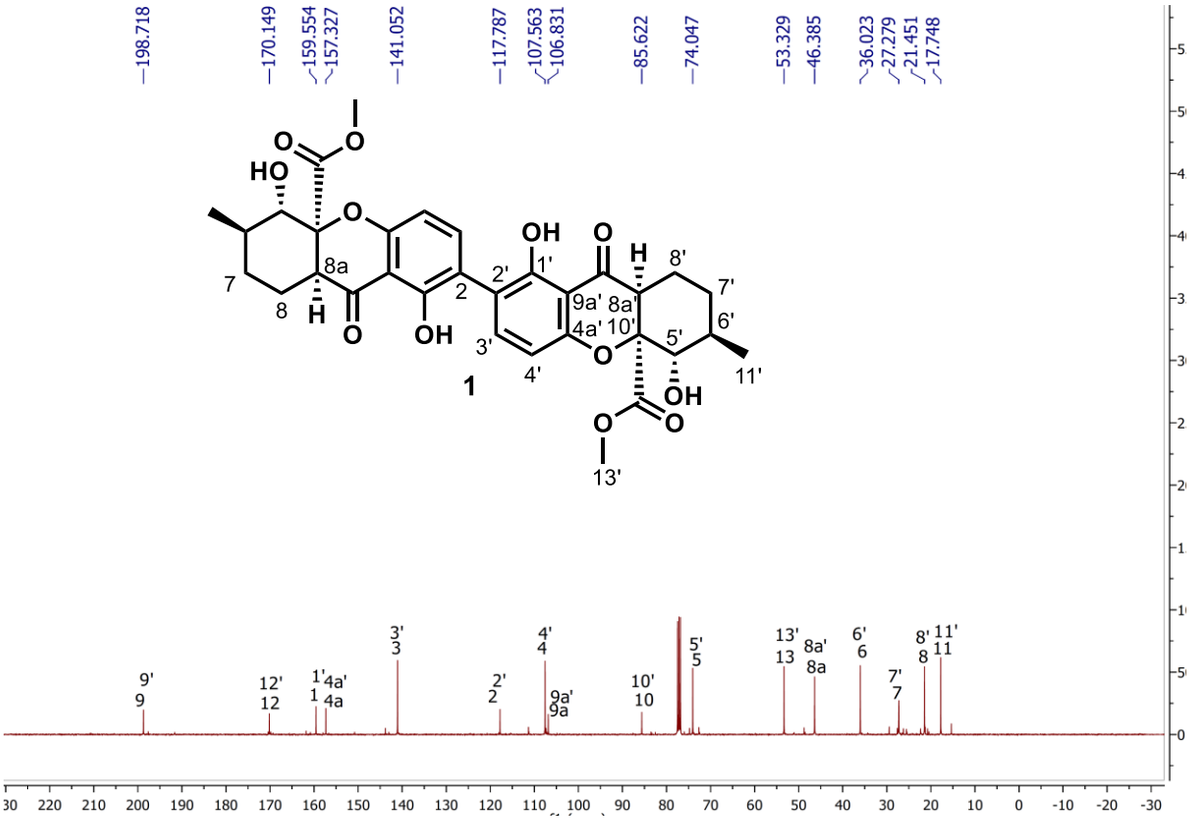

Fig. S5. The ^{13}C NMR spectrum of **1** in $CDCl_3$, 100 MHz.

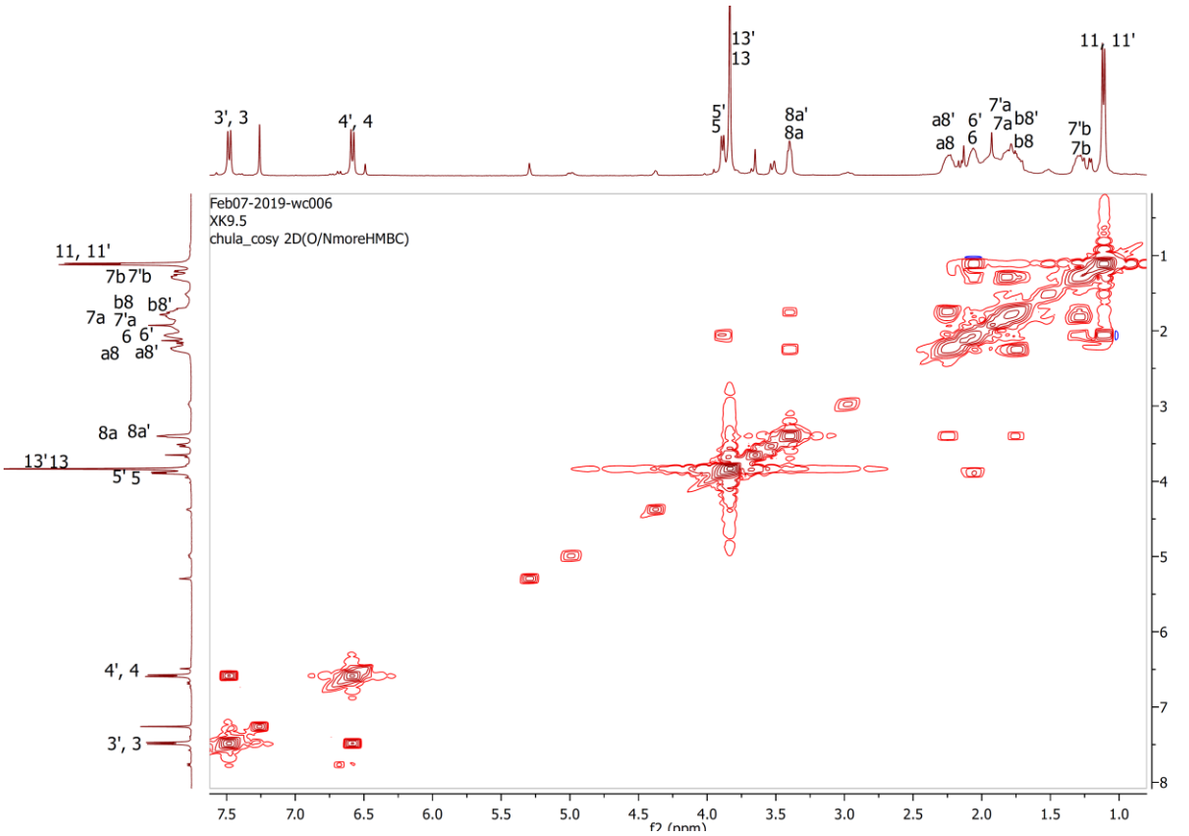

Fig. S6. The COSY spectrum of **1** in $CDCl_3$.

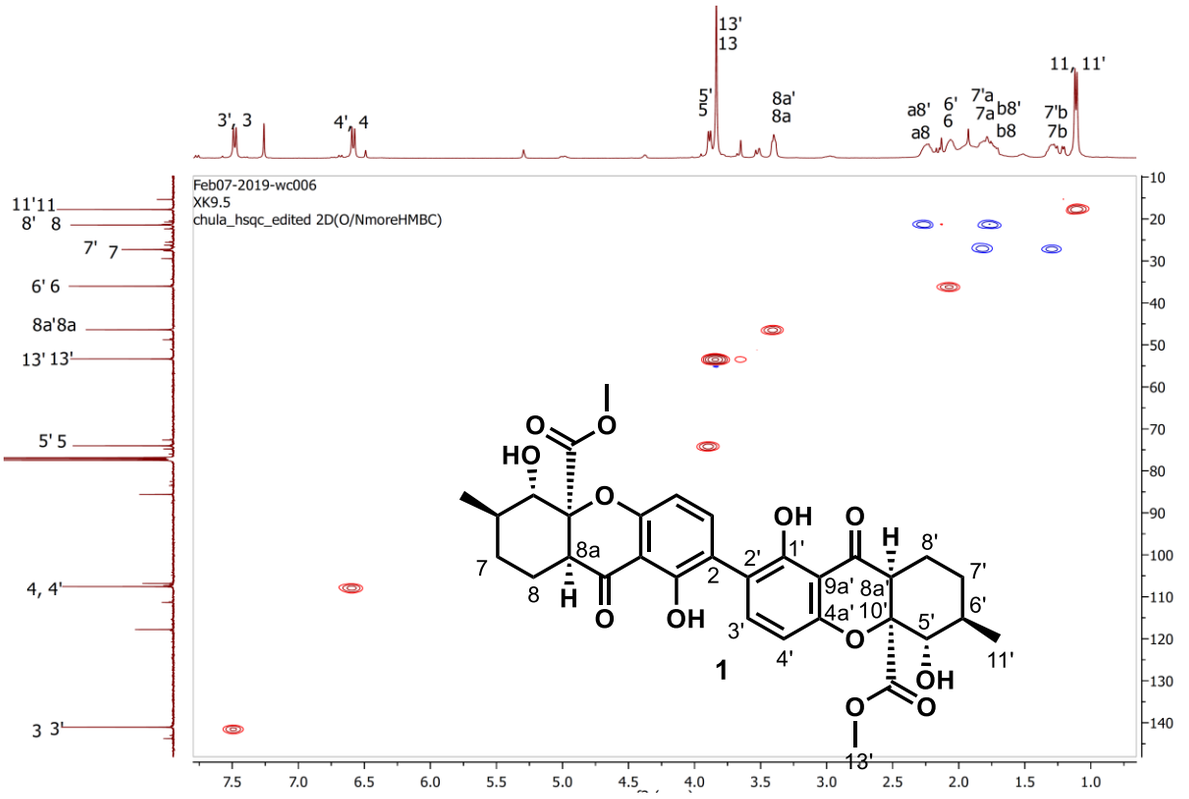

Fig. S7. The HSQC spectrum of **1** in $CDCl_3$.

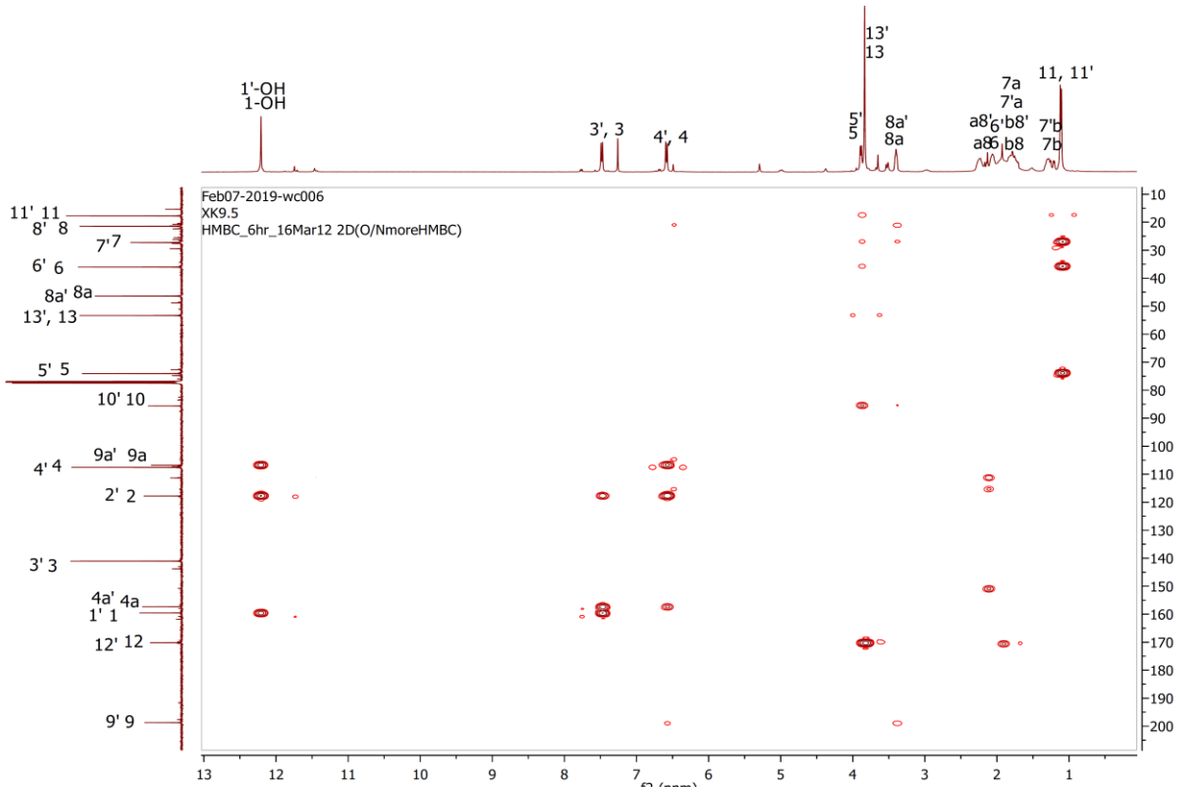

Fig. S8. The HMBC spectrum of **1** in $CDCl_3$.

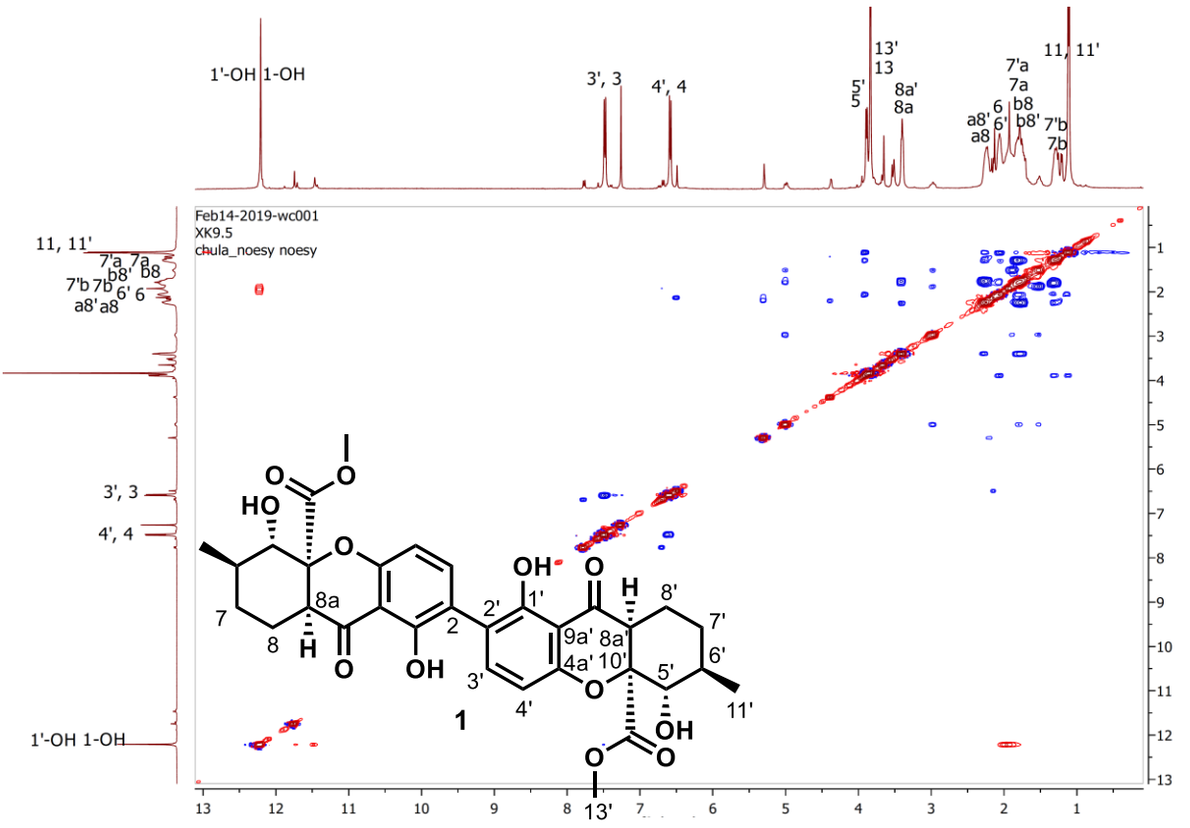

Fig. S9. The NOESY spectrum of **1** in $CDCl_3$.

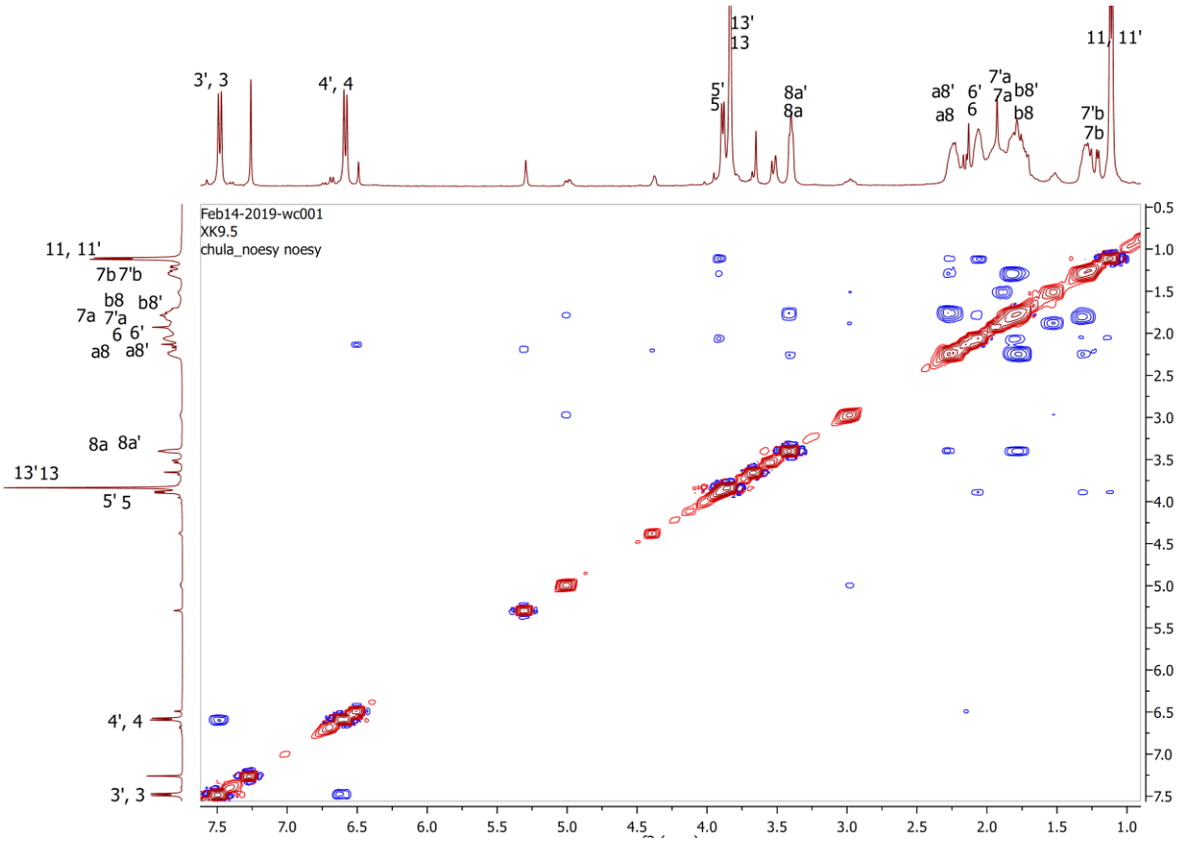

Fig. S10. The expanding NOESY spectrum of **1** in $CDCl_3$.

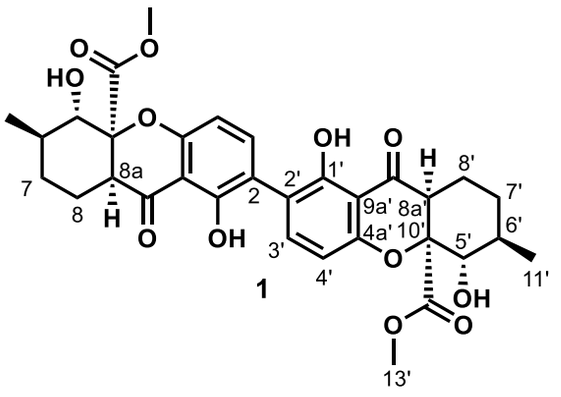

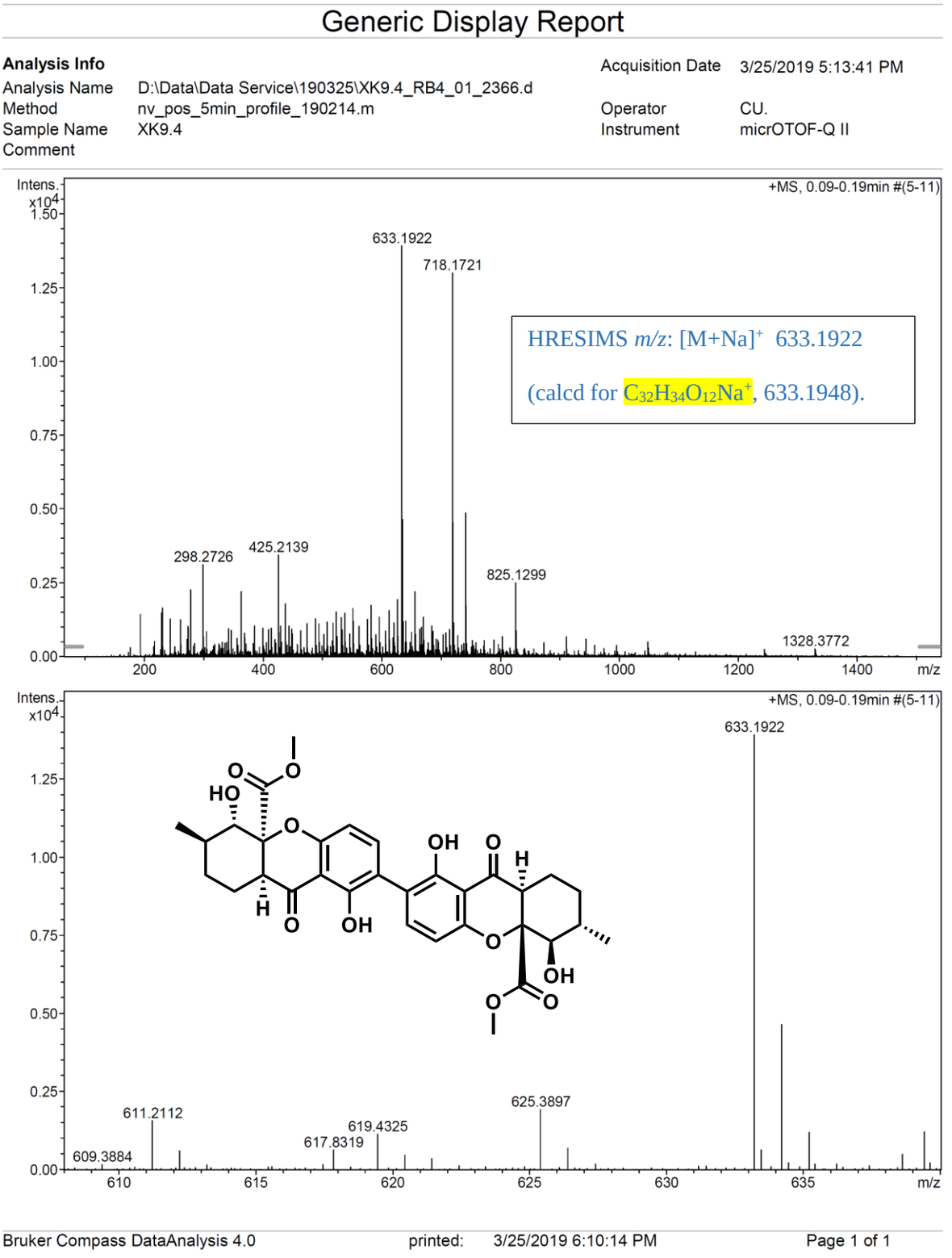

Fig. S11. The HRESIMS spectrum of **2**.

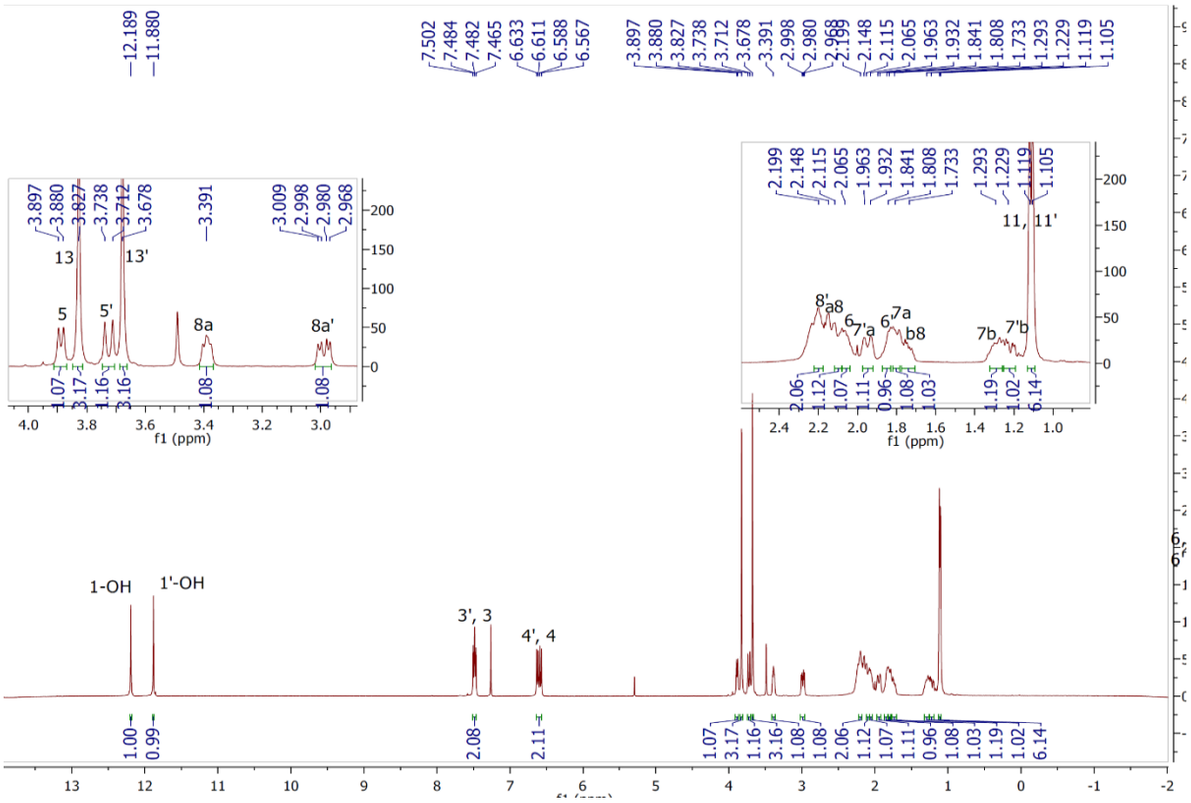

Fig. S12. The ^{1}H NMR spectrum of **2** in $CDCl_3$, 400 MHz.

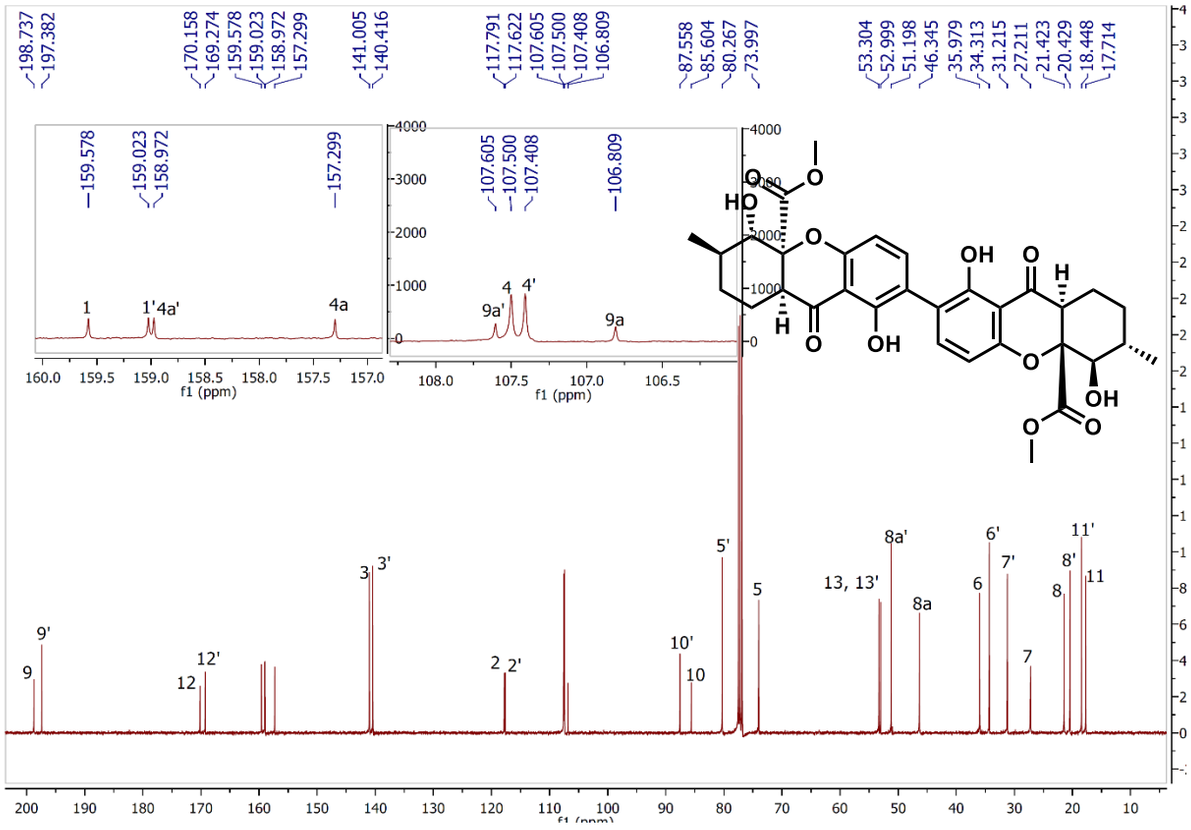

Fig. S13. The ^{13}C NMR spectrum of **2** in $CDCl_3$, 100 MHz.

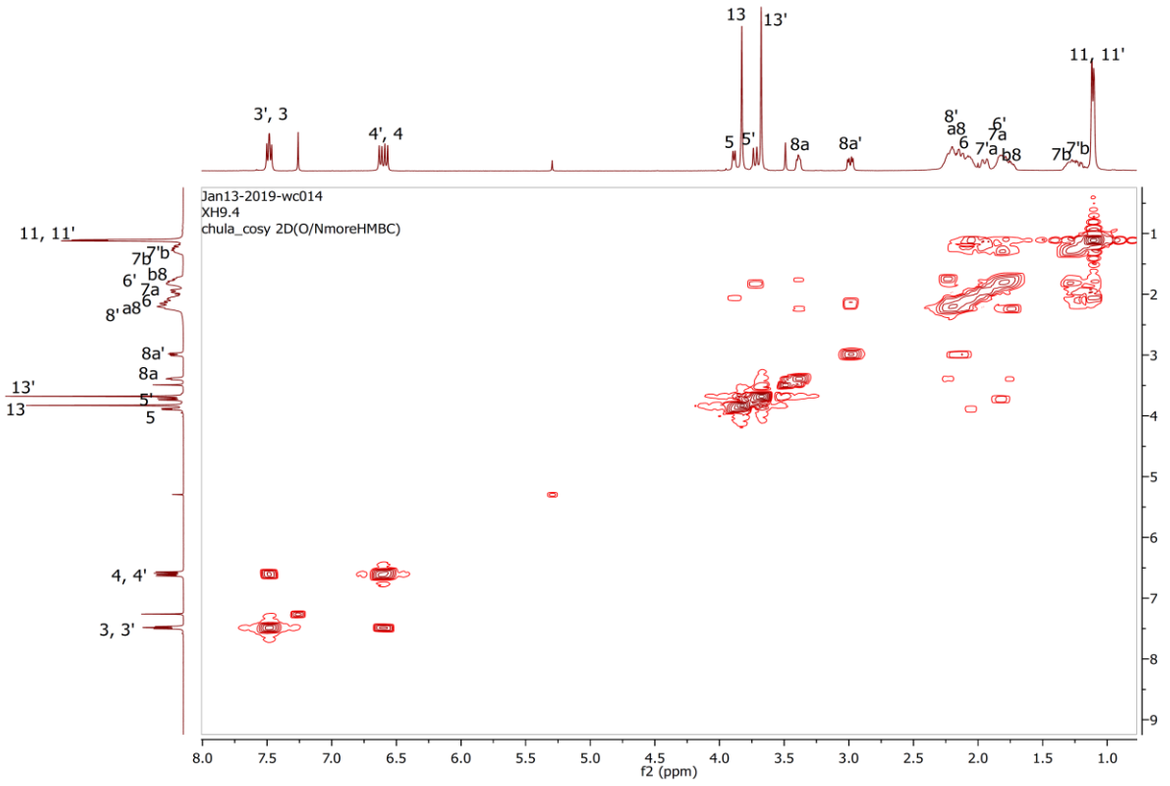

Fig. S14. The COSY spectrum of **2** in $CDCl_3$.

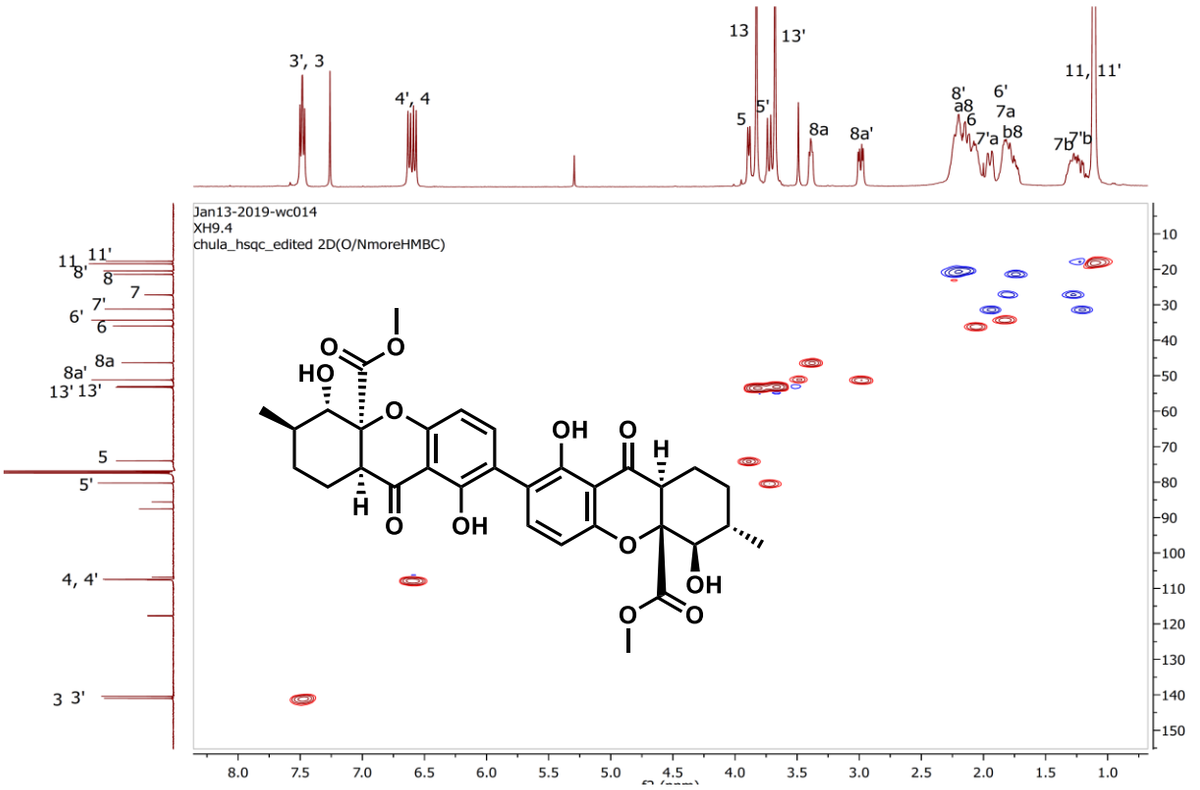

Fig. S15. The HSQC spectrum of **2** in $CDCl_3$.

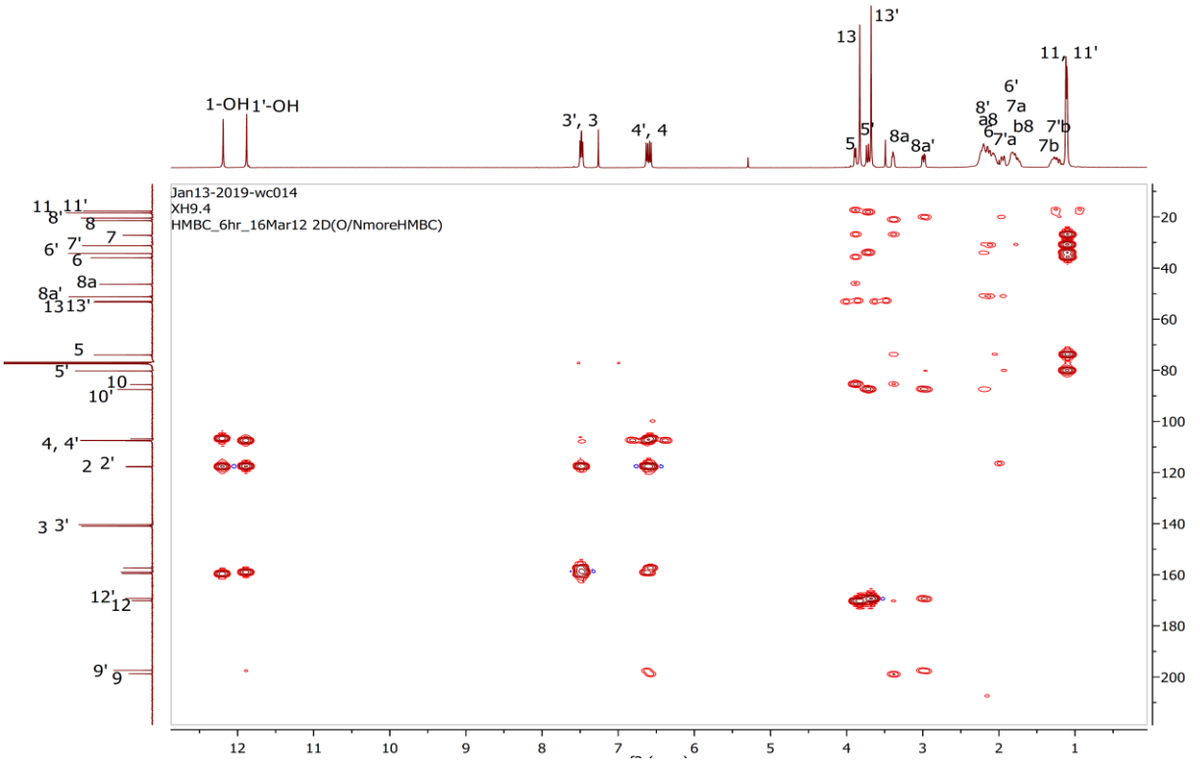

Fig. S16. The HMBC spectrum of **2** in $CDCl_3$.

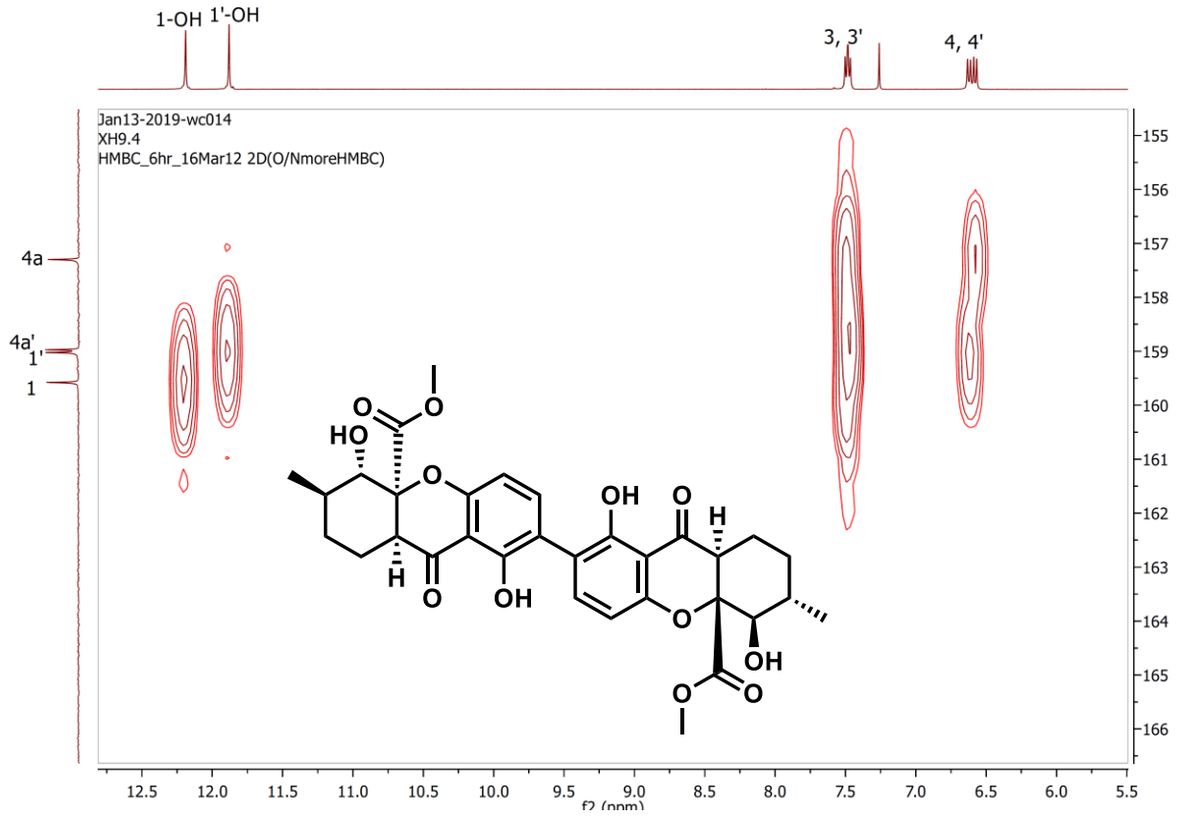

Fig. S17. The expanding HMBC spectrum of **2** in $CDCl_3$.

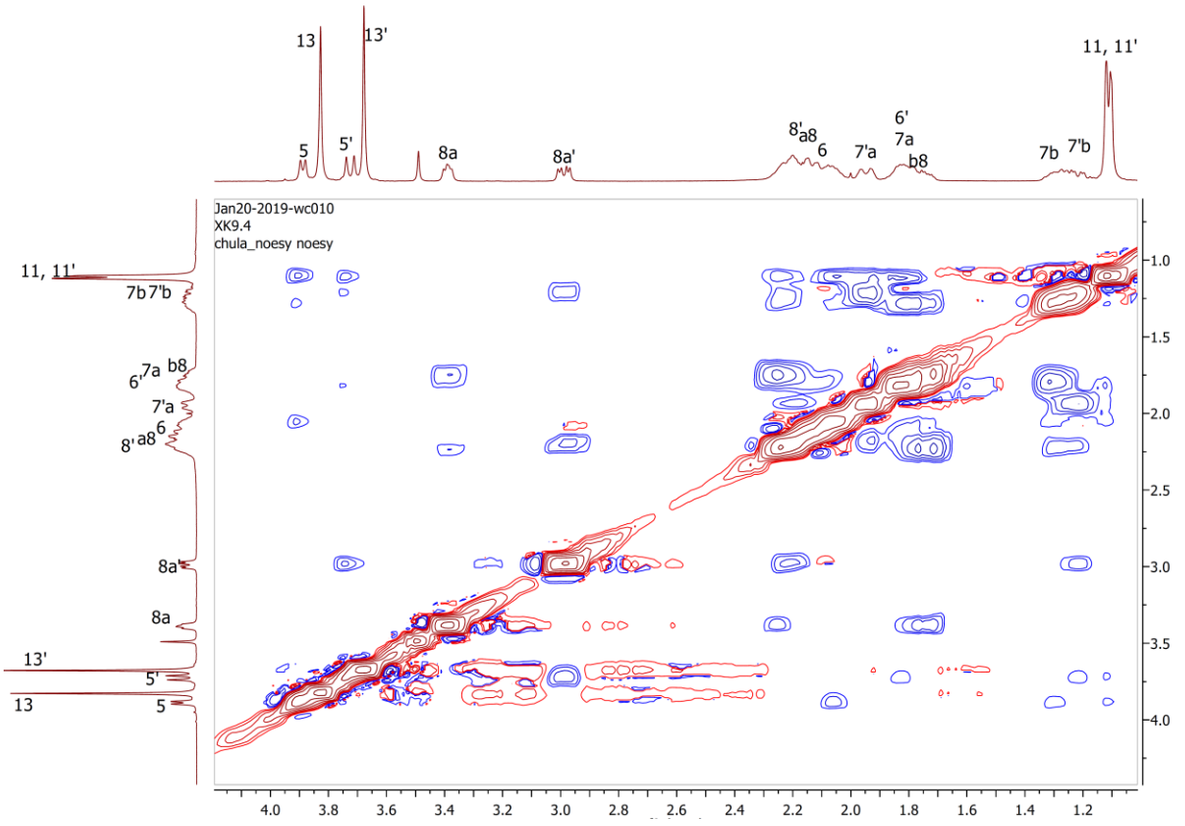

Fig. S18. The NOESY spectrum of **2** in $CDCl_3$.

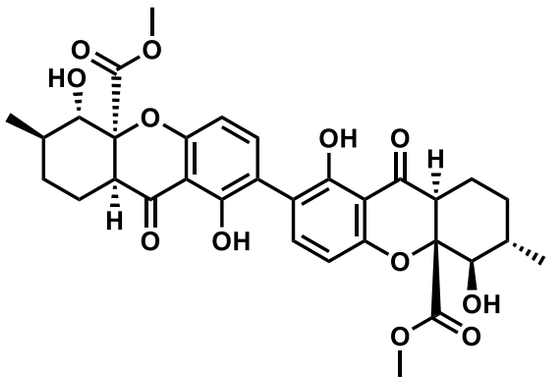

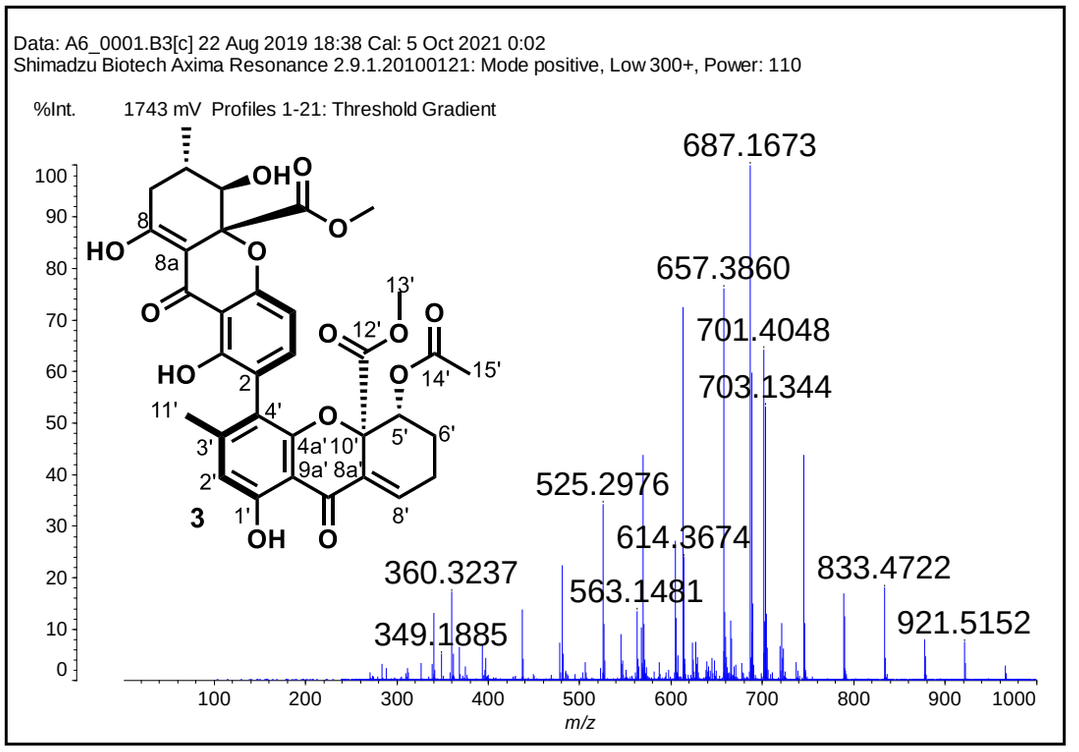

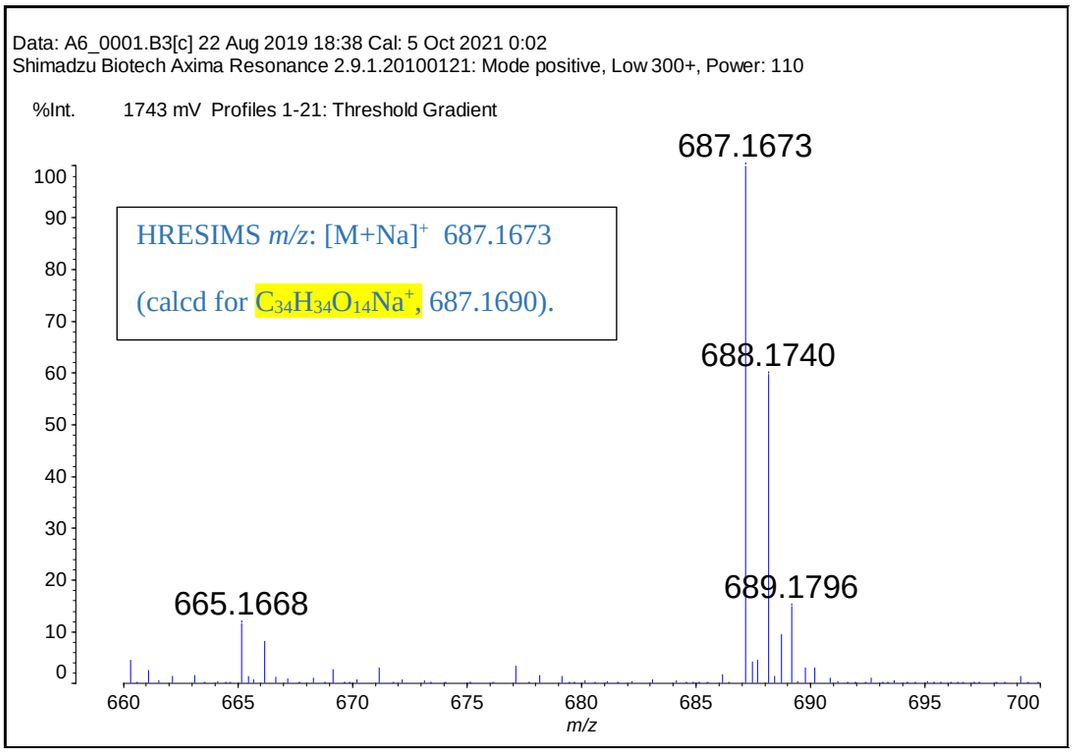

Fig. S19. The HRESIMS spectrum of **3**.

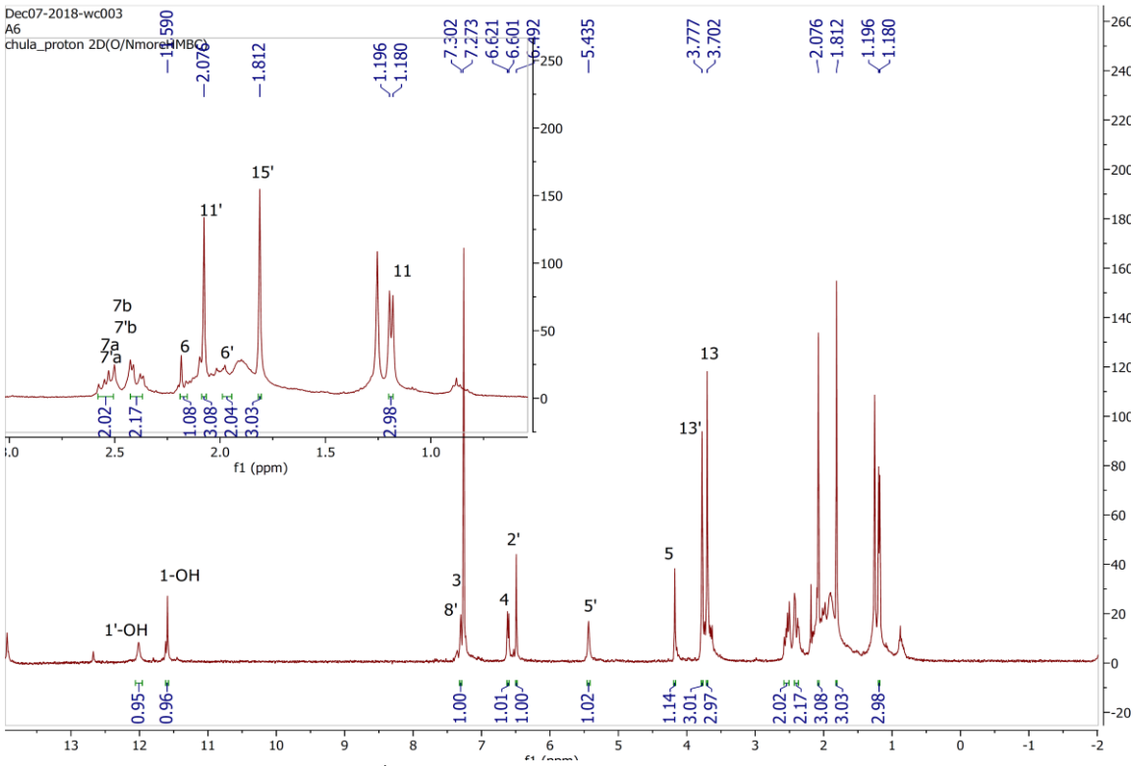

Fig. S20. The ^{1}H NMR spectrum of **3** in $CDCl_3$, 400 MHz.

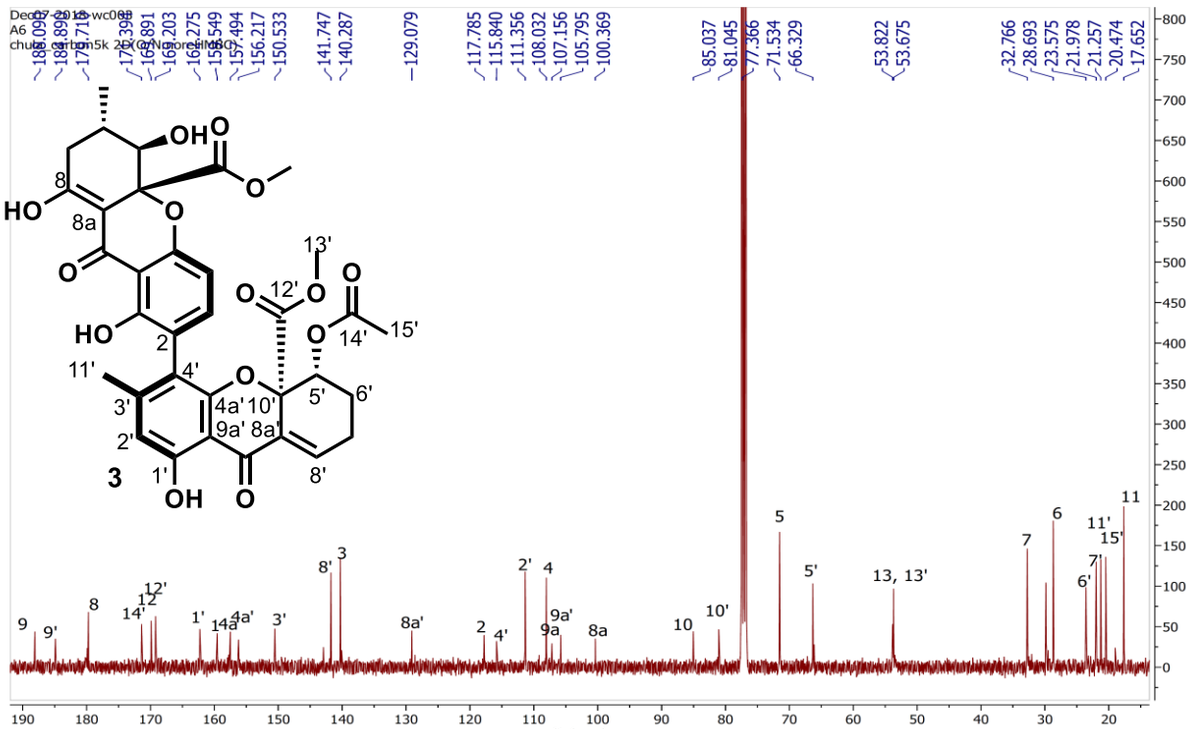

Fig. S21. The ^{13}C NMR spectrum of **3** in $CDCl_3$, 100 MHz.

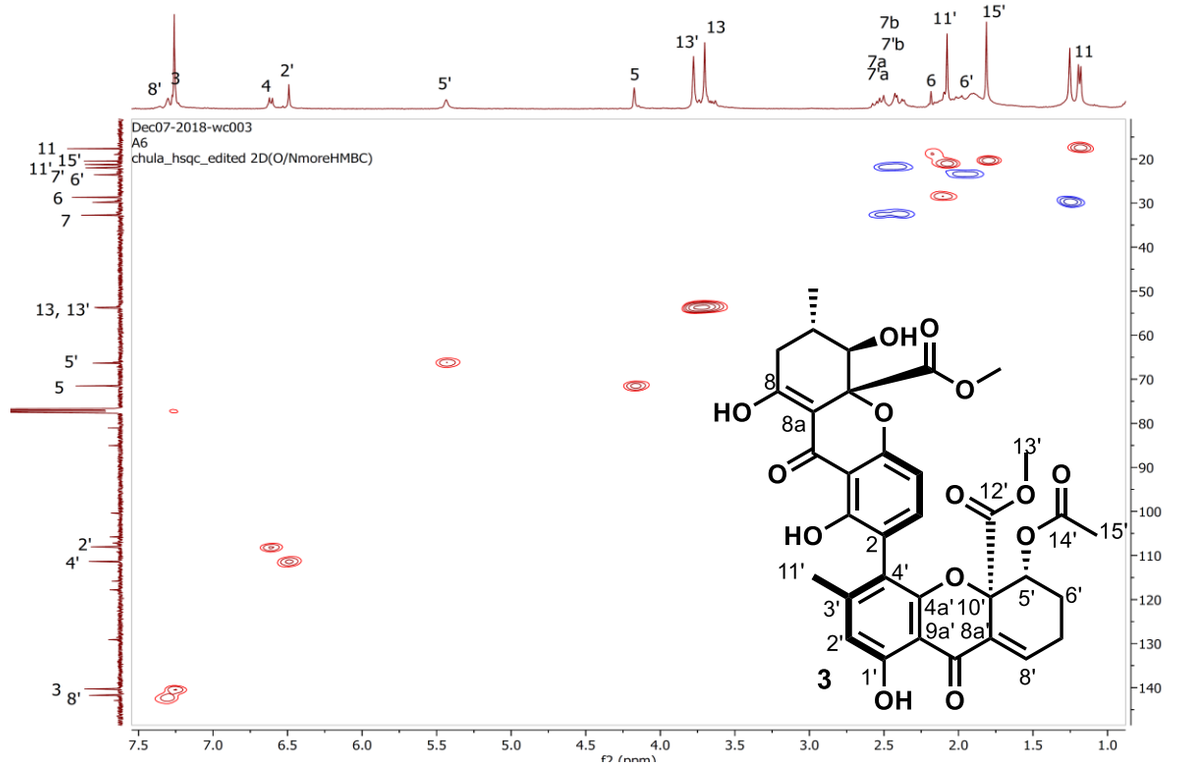

Fig. S22. The HSQC spectrum of **3** in $CDCl_3$.

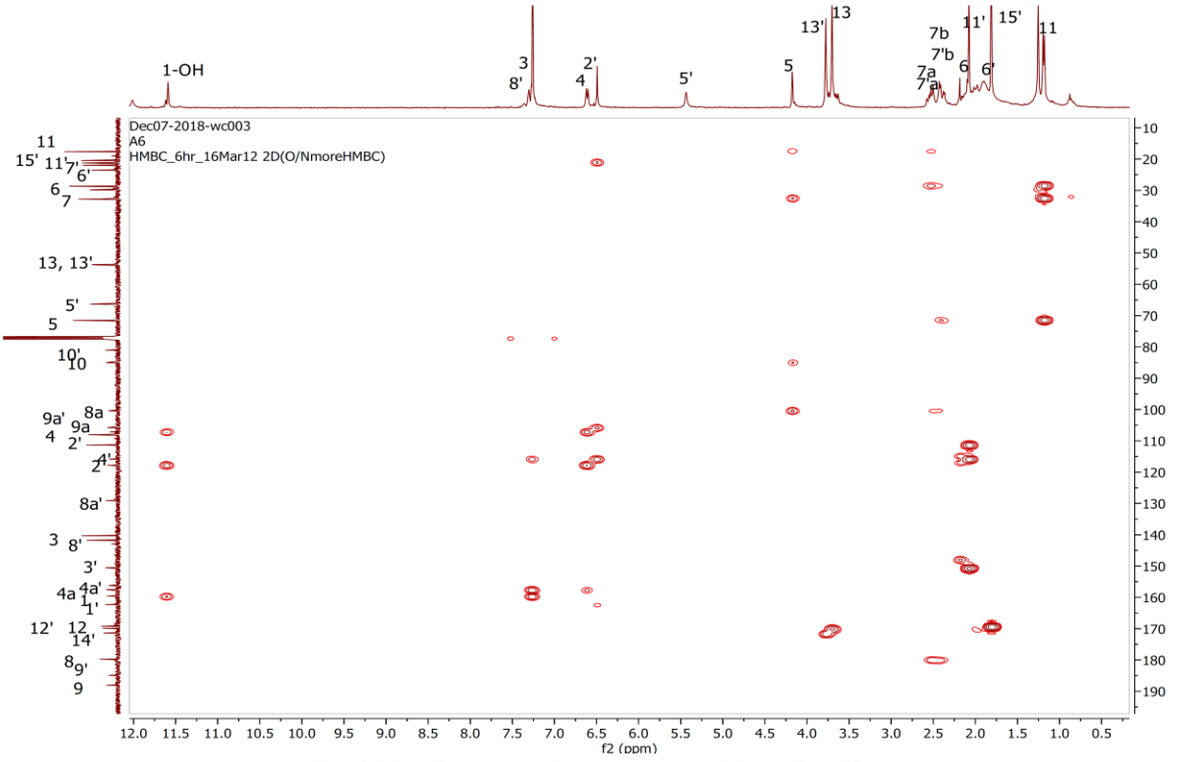

Fig. S23. The HMBC spectrum of **3** in $CDCl_3$.

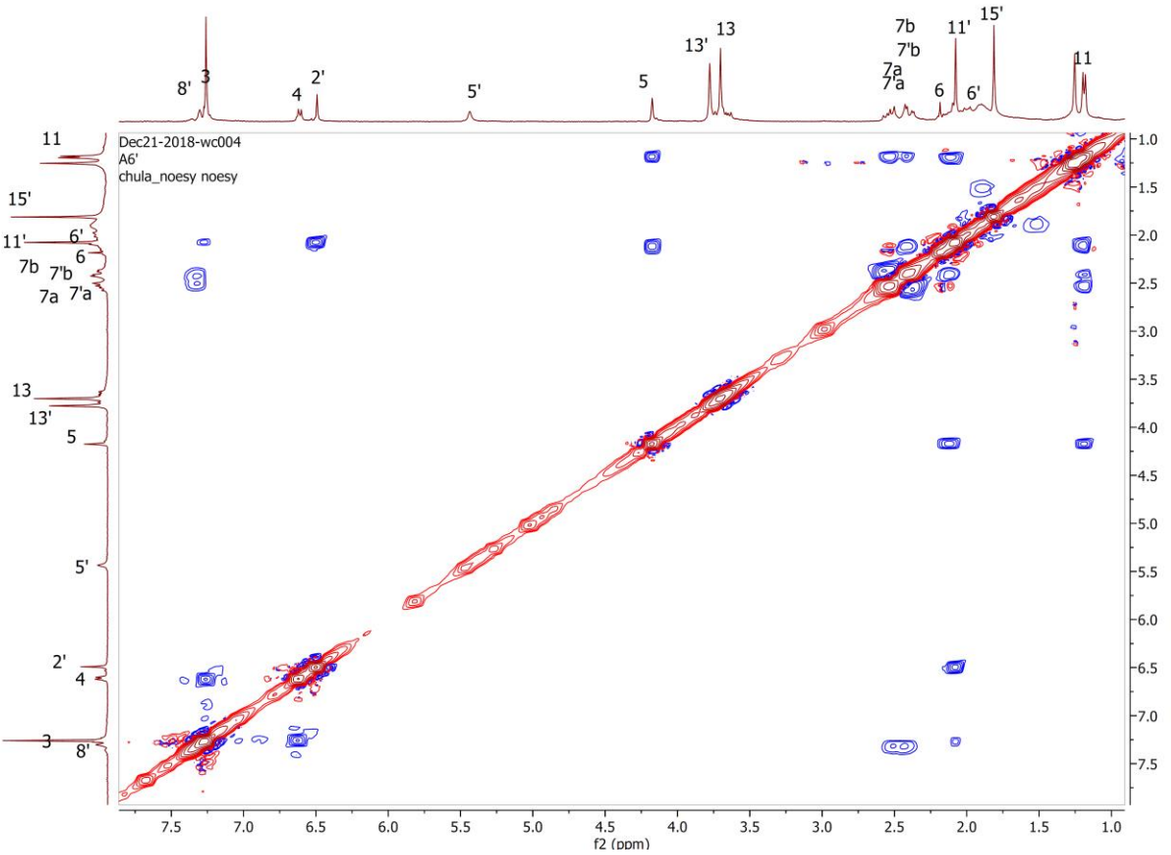

Fig. S24. The NOESY spectrum of **3** in $CDCl_3$.